# MODELLING OF ATOMIC NUCLEUS' STRUCTURE

Bondarev V.G., Migal L.V.

**Summary.** The structure of light atomic nuclei, such as hydrogen, helium and lithium nuclides, was studied based on the cluster approach. Atomic nuclei are formed as systems consisting of free and bound lovetons, as well as neutron electrons and electron-positron pairs. The work focuses on the mass of the atomic nucleus and its binding energy as the main basic characteristics. There were determined the mechanisms considered binding nucleons into clusters, as well as the main patterns of changes in binding energy depending on the structure of the nucleus.

As part of this study, atomic nuclei were visualized and the dependence of the nuclear binding energy on the number of lovetons, electron-positron pairs and neutron electrons was revealed. The possibility of forming a shell structure of an atomic nucleus consisting of cluster associations of α-particles has been shown. An algorithm for constructing the structure of the atomic nucleus is presented. The conditions for choosing the number of nuclear elements included in the atomic nucleus are determined. As additional results, an estimate of the binding energies of hypothetical hydrogen nuclides $^{8}$H and $^{9}$H was obtained, and their mass formulas were constructed. The charge radii of a number of hydrogen, helium and lithium nuclides have been calculated. The possibility of using the spiral structure of nuclei instead of the shell representation has been revealed. The nature of the occurrence of the binding energy of the atomic nucleus is explained. Comparison of the obtained values of binding energies and charge radii with experimental data allows us to assert an adequate approach to the formation of the structure of the atomic nucleus.
**Key words:** atomic nucleus, cluster model, binding energy, visualization, structure, loveton, nucleon, nuclide, neutron electron, electron-positron pair, nucleon pairing, charge radius.

## *INTRODUCTION*

The atomic nucleus is a multiparticle self-consistent system consisting of nucleons interconnected by nuclear interaction forces. Description of the properties of the nucleus based on the laws of interaction between nucleons is one of the most important problems of nuclear physics [1-3]. There are various models of atomic nuclei [4, 5] that describe the parameters of nuclei, including the interaction energies of nucleons. The development of nuclear models was carried out in two different directions. The first direction is characterized by the creation of "independent particle models", in which it is assumed that each nucleon moves in the average field of all other nucleons in the nucleus almost independently of each other. This group includes: the Fermi gas model, the potential well model, the nuclear shell model, and the generalized and optical models. The second direction is characterized by the creation of "models with strong interaction" [6]. In these models, the nucleus is considered as an ensemble of strongly interacting particles. This group of models includes: the liquid drop model, the cluster model, and the compound nucleus model.

The nuclear shell model [7] is widely used, in order to study the processes occurring in atomic nuclei. The theory of nuclear shells was developed by M. Goeppert-Mayer and I. Jensen for a single-particle model with a potential of three terms, including the spin-orbit interaction.

Most of the proposed nuclear models are based on a fundamental approach, which serves as the main guideline for constructing phenomenological models. However, its application is severely limited, and therefore approximate methods have become widespread. The main approximate microscopic method is the mean field method [8]. The mean field method, or Hartree-Fock method, makes it possible to describe the self-consistent nuclear field through studies of 2-particle interactions. Based on this concept, it was possible to explain why the properties of nuclei with similar numbers of protons and neutrons are very different from each other. Calculations in mean-field models make it possible to estimate binding energies for individual nuclei, and the accuracy of predictions ranges from 0.3 to 1 MeV for the total binding energy [9, 10].

Using the Hartree-Fock method, it is possible to calculate the masses, radii and distributions of nucleons, as well as other nuclear properties. So, at work [11] the calculation of the masses of nuclei between the proton and neutron boundaries of existence is given; when updating the array of empirical data on masses, refined calculations are made using the Skyrme potential [12]. In this case, the standard deviation in calculations for binding energies does not exceed 0.55 MeV. However, we note that the disadvantages of most of these models are their

phenomenology, the lack of structural representations, and the nature of intranuclear interactions is not considered.

In a number of models, the atomic nucleus is considered as a system consisting of individual nucleons that form compact structures of two or more particles inside the nucleus [13]. Depending on the ratio of the number of protons and electrons, various constructions are possible, called clusters. To date, many theoretical techniques have been developed to study the phenomenon of nuclear clustering [14]. In a simple cluster model, it is believed that the atomic nucleus consists of two structureless fragments, the properties of which coincide or are close to the properties of the corresponding nuclei in a free state [15]. The cluster structure is especially clearly manifested in light nuclei.

The stability of an atomic nucleus is characterised by its binding energy. Here, the binding energy is understood as the minimum amount of energy that must be expended to completely separate the atomic nucleus into individual nucleons. Another interpretation of the binding energy is possible, based on the reverse process, i.e., it represents the energy released during the fusion of free nucleons into the atomic nucleus [16].

The experimentally established distribution of binding energies over mass numbers in the nucleus has the following characteristic features [17, 18]:

1. For kernels with small values mass number the specific binding energy tends to increase.

2. For heavy nuclei, the specific binding energy is lower than for medium nuclei, and with increasing mass number there is a decrease in its value.

3. For nuclei with the same numbers of protons $Z$ and neutrons $N$, the specific energy is higher than for atomic nuclei with the same value mass number $A$, but with numbers of nucleons different from equality.

4. Even-even nuclei have, on average, higher specific binding energies than odd-even or even-odd ones, and odd-odd ones have even lower specific binding energies.

Theoretical explanation for this behavior specific binding energy gives the liquid drop model [19]. Taking into account all the listed properties leads to the semi-empirical Weizsäcker formula

$$E_b = a_1 A - a_2 A^{2/3} - a_3 Z^2 A^{1/3} - a_4 (A/2 - Z)^2/A + a_5 A^{-3/4}. \quad (1)$$

where $a_1$-$a_5$ are empirical coefficients; $E_b$ is the binding energy; $A$ is the mass number; $Z$ is the charge number.

The coefficients in formula (1) are selected from the conditions of the best agreement between the model distribution curve and the experimental data on binding energies. Equation (1) can approximately describe the binding energy of nucleons as a function of mass number $A$ for all nuclides except the lightest nuclei, with $A < 20$ [20]. The greatest discrepancy between the experimentally measured values of nuclear binding energy and calculations using the Weizsäcker formula is observed in the region of magic numbers [22]. This is explained by the fact that the droplet model does not take into account the inhomogeneities in the distribution of nuclear matter caused by the shell structure of atomic nuclei [21].

The first attempt to correct the Weizsäcker mass formula by taking into account microscopic effects was made back by Myers and Świątecki [23]. The effects of the shell structure were manifested in the fact that the position of the levels of the single-particle spectrum deviated from the levels in the uniform spectrum. The shell correction was calculated as the difference between the energy levels of the shell model and the liquid-droplet (statistical) Fermi gas model. To improve the quality of predictions, in addition to the shell correction, the Wigner term was additionally introduced, which is associated with the special stability of nuclei with the same numbers of protons and neutrons [24].

Weizsäcker's formula was the first step towards a complete description of nuclear matter. Currently, a large number of model calculations of binding energy have been proposed. Models

for analytical calculation of binding energies can be divided into microscopic, macro-microscopic, and phenomenological estimates based on local mass ratios [25]. Local mass ratios are arithmetic expressions that combine the binding energies of several nuclei close to each other on the nuclide map [26]. Based on the above considerations, the FRDM (Finite Range Droplet Model) model was created [27].The total nuclear energy in this model depends not only on the charge of the nucleus and the number of neutrons, but also on the shape of the nuclear system. In total, the FRDM model has 10 independent parameters, which must be determined using an array of experimental data on nuclide masses. In the modern FRDM model [28] the error is 0.56 MeV for 2194 nuclei from $^{16}$O to $^{264}$Hs, and for the region $N > 64$ – 0.35 MeV, which makes the model comparable in accuracy to microscopic methods.

The structural approach is also important, which, on the one hand, uses visual visualization, and on the other, is based on values determined by experimental methods [29]. Usually, the nucleus of an atom is usually depicted as an ellipsoidal dense packing of nucleons [30]. However, recently studies have appeared in which the core structure is a fragment of some lattice [31, 32].

In the process of studying the atomic nucleus, it became clear that the structure of a neutron or proton can change when the particle is bound in the atomic nucleus. Thus, it was discovered that the internal structure of nucleons depends on their environment [33]. That is, the structure of a nucleon in empty space is different from its structure when it is located in an atomic nucleus. However, despite theoretical and experimental work, the reason for this modification remains unclear.

Starting with the works of J. Wheeler, K. Wildermuth and Y. Tang [34], which laid the foundations for studying the cluster properties of nuclear systems, it turned out that using the microscopic method it is possible to describe a wide range of physical phenomena, for example, static clustering and cluster decays, from a unified point of view, and also make significant progress in the study of processes in which such systems are involved.

Consideration of the structure of the atomic nucleus shows that independent groups of clusters with characteristics close to the properties of individual free nuclei can be realized in the nucleus. Previously existing ideas about clusters stably existing in the nucleus were replaced by the understanding that in the process of almost independent movement of nucleons in the nucleus, virtual subsystems in the form of clusters are formed and destroyed [35]. Therefore, we can only talk about the probability of the existence of one or another cluster channel. However, if this probability is relatively high, you can use a single-channel cluster model, which in many cases turns out to be a good approximation to the situation actually existing in the kernel. Such a model makes it relatively easy to perform any calculations of nuclear characteristics, even in those systems where methods for solving the many-body problem are either very cumbersome in numerical execution or do not lead to specific quantitative results at all.

Problems associated with the study of the cluster properties of the atomic nucleus have recently attracted special attention. The properties of clusters and the specifics of their interaction are reflected in the observable characteristics of the system as a whole and its reactions to various external influences. The experimental results for determining the binding energy of the nucleus also contain “pulsations” at a level of 1-2 MeV. Thus, the neutron separation energy for some nuclides periodically increases when the number of neutrons becomes even, and decreases when their values are odd. The difference in binding energies between even and odd nuclei indicates the presence of pairing forces in atomic nuclei [36]. Based on this consideration, as the goal of the presented work, one can choose to construct the nucleon structure of the nucleus based on the cluster approach and estimate the binding energies based on the available experimental data. At the same time, the problems of analyzing the structure of a number of nuclides are solved, with the possibility of subsequent formation of the spatial structure of the atomic nucleus.

## *1. RESEARCH OBJECTIVE*

Let us consider the problem of constructing the structure of the atomic nucleus by

studying the relative arrangement of nuclear elements: lovetons, electron-positron pairs and neutron electrons for light nuclei, and also show the possibility of layer-by-layer placement of α-particles in accordance with the shell model of the nucleus. All calculated values of the parameters of nuclear elements are presented in Table 1 [37].

Table 1

Calculated data on nuclear elements and their binding energies

| Particle | Mass (meV) | Type connect | Energy connect (meV) |
|---|---|---|---|
| Loveton, *L* | 882.158477726 | *LL* | 6.18094291005 |
| Electron, *e* | 0.51099895 | *Le* | 0.78127053419 |
| Neutrino, *ν* | 0.00106285981 | *ee* | 0.95644605733 |

**Note**. For neutrino, the value of the reduced mass is given. Designations: *LL* –loveton-loveton; *Le* – loveton electron; *ee* – electron-electron (positron).

To carry out the calculations, we use the original array of experimental data, which represents the binding energies of the Atomic Mass Evaluation AME 2022 nucleus [38], as well as data on charge radii [39], necessary for the targeted formation of structure and visualization of atomic nuclei.

When constructing structures of atomic nuclei, it is necessary to adhere to a number of conditions and restrictions:

1. In the vast majority of cases, modeling will not consider the Coulomb repulsion forces acting between protons in the nucleus.

2. The structure of the nucleus will be modeled by a system of nucleons consisting of combinations of lovetons, neutron electrons and electron-positron pairs.

3. Due to the closeness of the binding energies of neutron electrons and electron-positron pairs, an exchange of bonds between these nuclear elements is possible.

4. The proposed method for forming the structure of a nucleus will be based on clustering analysis, that is, on the representation of a nucleus consisting of a collection of light nuclei and individual nucleons, considered as clusters forming a compound nucleus.

5. The main geometric objects of the model of atomic nuclei will be free lovetons, which, together with bound lovetons, electrons and electron-positron pairs, model individual light nuclei. In this case, bound lovetons perform the function of creating cells of the nuclear framework into which free lovetons are embedded.

6. To visualize the structure of the nucleus, you should build its diagram by filling the nuclear frame with the appropriate number of nuclear elements, choosing the number of frame cells and correctly placing each free loveton in its cell. Next, you should write down a mass formula that determines the type of nucleus in all areas of the nuclear diagram.

7. The effect of nucleon pairing can only occur in combined nuclei.

8. The combination of nucleons to form an atomic nucleus can be caused by dipole attraction induced by electron-positron pairs that make up the nucleons [37].

9. The proposed model of the atomic nucleus does not require the introduction of a hypothesis about the presence of quark objects. The mass of a neutrino is a fairly small value, so we will also exclude this particle from consideration when carrying out the process of formation of an atomic nucleus.

According to the rules defined above, using computer modeling, spatial models can be built for all atomic nuclei. When conducting research taking into account this approach, formulas for determining the mass of the *i*-th atomic nucleus $M_i$, as well as binding energy $E_b$ can be represented in the following form

$$M_i = N_L m_L + N_e m_e + N_{LL} E_{LL} + N_{Le} E_{Le} + N_{ee} E_{ee} \quad (2)$$

where $E_{LL}$, $E_{Le}$, $E_{ee}$ are the energies of *LL*-, *ee*- and *Le*-bonds in the nucleus; $N_L$, $N_{LL}$, $N_{Le}$, $N_{ee}$ are respectively, the number of lovetons, *LL*-, *ee*- and *Le*-bonds in the nucleus; $m_L$, $m_e$ are loveton and electron masses.

$$E_b = N_p m_p + N_n m_n - M_i \quad (3)$$

where $N_p$, $N_n$ is number of protons and neutrons in the nucleus; $m_p$, $m_n$ are experimental values of proton and neutron mass.

As a basis for constructing composite atomic nuclei, we will take the structural schemes of the proton and neutron (Fig. 1), as well as their mass formulas

$$M_p = m_L + 2m_e + 8E_{LL} + E_{ee} + 6E_{Le} \, . \quad (4)$$

$$M_n = m_L + 3m_e + 8E_{LL} + E_{ee} + 7E_{Le} \, . \quad (5)$$

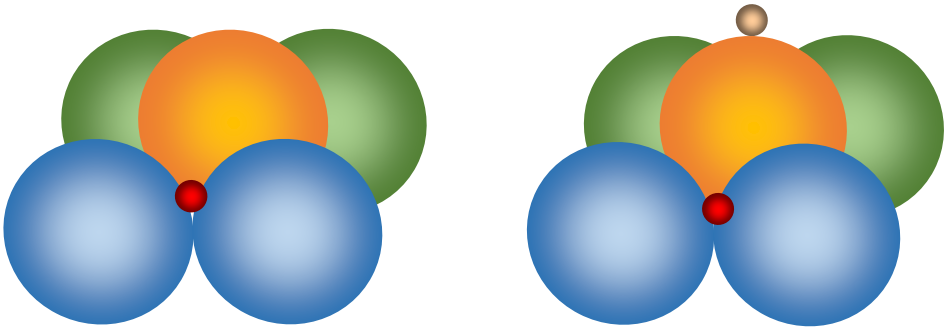

*a*) *b*)

Fig. 1 – Schemes of the structure of the nucleons:
*a*) proton; *b*) neutron
– bound lawton; – bound antiloveton; – free loveton;
– electron; – electron-positron pair

When determining the structural composition of atomic nuclei, we will consider the binding energy of the nucleus as the main criterion. Analysis of the change in binding energy when adding nuclear elements will allow us to estimate the magnitude of the change in the number of *LL* bonds, and an approximate assessment of the data on the number of *ee*-and *Le*-bonds can be carried out by calculating possible combinations of elements in the nucleus. Auxiliary analysis based on these relationships of linear dependences on the mass number will confirm the correctness of determining the structural composition of the selected nucleus.

The mass estimates in the proposed method can be obtained using a step-by-step algorithm. We select an array of experimental data on the binding energies of nuclei, and use formula (2) to calculate the binding energy at the first step. If the calculation is performed by variations of the parameters in formula (2), the obtained estimates are averaged. Thus, for each new nuclide it is possible at one step to obtain from 1 to 4 estimates of the possible number of nuclear elements. The procedure is repeated until one set of nuclear elements is selected. Thus, more accurate results can be achieved if one takes into account possible changes in the binding energies of electron-positron pairs and neutron electrons with lovetons.

## *2. MODEL FORMATION*

### *2.1 HYDROGEN NUCLIDES*

**Hydrogen-2 ($^2$H).** For a deeper understanding of the structure of the nucleus, we will first understand the structure of the simplest compound nucleus of hydrogen – $^2$H (deuteron), which is a deuterium nucleus. The results obtained, in terms of explaining the composition and structure of the deuteron, will in the future allow us to determine the general principles for constructing the

structure of atomic nuclei.

According to modern concepts, a deuteron is formed by the union of two nucleons: a proton and a neutron. In the deuteron, the proton and neutron can be united through the removal of two bound lovetons from their common composition. The loss of the two lovetons results in a reduction in the number of *LL*-bonds by three bonds. However, combining a proton with a neutron adds two new bonds to the structure of the resulting deuteron, which reduces the total number of *LL*-bonds by only one unit. In this case, two different structural states are formed (Fig. 2).

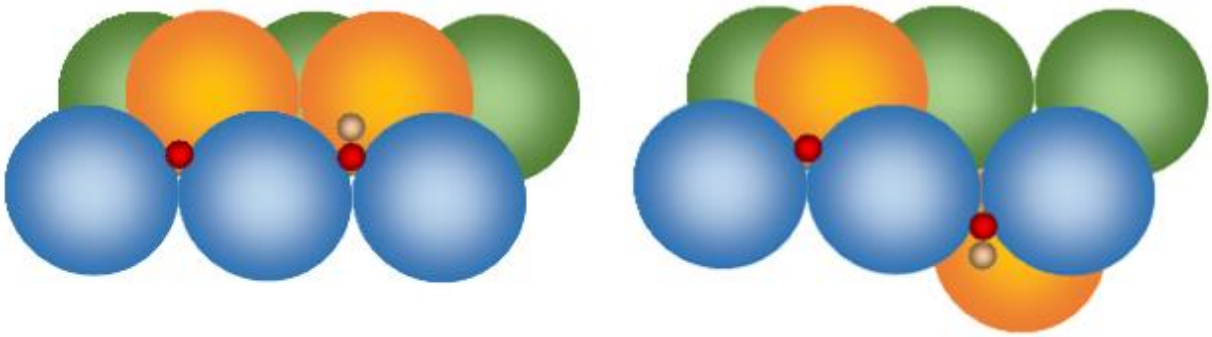

*a*) *b*)

Fig. 2 – Schemes of the structure of the deuterium (deuteron) nucleus:
*a*) linear placement of lovetons; b) diagonal placement of lovetons

The structural patterns that can be formed from a neutron and a proton are obtained when the free lovetons of the proton and neutron are combined linearly (Fig. 2a), and also when they are placed diagonally relative to the position of the bound lovetons (Fig. 2b),

Regardless of the type of structural diagram chosen, this representation of the deuteron allows us to write the only mass formula for the deuteron

$$M(^2H) = 2m_L + 5m_e + 15E_{LL} + 7E_{ee} + 12E_{Le}. \quad (6)$$

In formula (6), the number of *LL*-bonds is the sum of the number of bonds between bound lovetons, determined by the value: $N_{LL}$ = 7, as well as the value of these bonds between free and bound lovetons: $N_{LL}$ = 8.

The total number of electrons and positrons included in the deuteron is numerically equal to: $N_e$ = 5. The number of *ee*-bonds in this case is calculated through the total number of possible bonds between particles in electron-positron pairs, determined through the number of combinations, with the addition of one neutron electron bond : $N_{ee}$ = 7.

The number of *Le*-bonds in a deuteron is determined by the number of these bonds between particles in electron-positron pairs and the lovetons in contact with them. For each such particle there are three bonds, therefore, the total number of *Le*-bonds will be equal to: $N_{Le}$ = 12.

The presence of a bond between a neutron electron and an electron-positron pair does not allow the occurrence of $\beta$-decay, and the loss of an *LL* bond does not allow for nucleon decay. For these reasons, the deuteron can be classified as a stable nucleus.

**Hydrogen-3 ($^3$H).**When a second neutron is added to the deuteron, the nuclide $^3$H (triton) is formed – a tritium nucleus (Fig. 3).

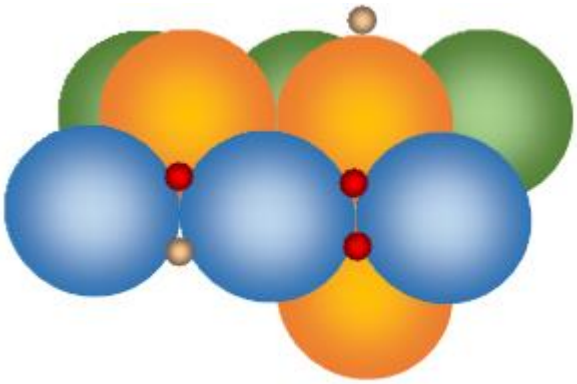

Fig. 3 – Scheme of the structure of the tritium (triton) nucleus

This diagram represents a structure consisting of a deuterium nucleus, which is combined with a neutron added to it. In this case, the added neutron completely loses the bound lovetons included in its composition. In this case, the number of *LL*-bonds increases to the following value: $N_{LL}$ = 20, including seven *LL*-bonds between bound lovetons, 12 bonds between free and bound lovetons, as well as the appearance of one additional *LL*-bond due to the effect of neutron pairing. The number of *ee*-bonds, taking into account the number of combinations between particles of electron-positron pairs, as well as the possible inclusion of one of the neutron electrons in their composition, gives us 21 *ee*-bonds. Note that the number of *Le*-bonds is equal to 19. However, if we assume that one of the *ee*-bonds of a neutron electron is also converted into *Le*-bond, then their number is equal to: $N_{Le}$ = 20. The same value will be represented by counting *ee*-bonds: $N_{ee}$ = 20. This scheme is energetically more favorable than the simple addition of a neutron to a deuteron; therefore it is the one that most closely matches the triton binding energy. Accordingly, the mass formula will have the form

$$M(^3H) = 3m_L + 8m_e + 20E_{LL} + 20E_{ee} + 20E_{Le}. \quad (7)$$

Thus, the triton is unstable because one of the neutron electrons has only one *Le*-bond, which can lead to $\beta$ decay.

**Hydrogen-4,5,6,7 ($^{4,5,6,7}$H).** All subsequent hydrogen nuclides decay directly into $^3$H (triton) and a series of neutrons. The instability of these nuclides indicates the absence of common *LL* bonds between triton and neutrons. Consequently, these particles form hydrogen nuclides only due to the presence of nuclear forces, as well as some change in the number of *ee*- and *Le*-bonds. Based on the above assumptions for $^4$H, the number of all bonds can be estimated by simply summing the bond data for the triton and the neutron attached to it. As a result, we will get the following values: $N_{LL}$ = 28; $N_{ee}$ = 21; $N_{Le}$ = 26, with the total number of electrons and positrons equal to $N_e$ = 11.

To clarify the summed values for $^4$H, we will use the known value of the binding energy obtained experimentally [37]. Correcting this formula taking into account the binding energy shows only an increase in *Le*-bonds to the value: $N_{Le}$ = 29. Consequently, neutron electrons, in the process of attaching a neutron to a triton, began to interact not only with their own free lovetons, but also with neighboring free lovetons, which leads to the appearance of three additional *Le*-bonds. This fact allows us to write the following final formula for $^4$H

$$M(^4H) = 4m_L + 11m_e + 28E_{LL} + 21E_{ee} + 29E_{Le} \quad (8)$$

The corresponding values for all subsequent hydrogen nuclides are calculated in a similar way. We only note the appearance of possible transitions in the number of *ee*- and *Le*-bonds, as well as the absence of pairing of hydrogen nucleons during the addition of neutrons. So, for hydrogen-5 this is an additional increase in the number of *ee*-bonds by one to the value $N_{ee}$ = 23. For hydrogen-6 there is an increase in not only *ee*-, but also *Le*-bonds by one as well. Hydrogen-7 has no additional bonds. The analysis carried out allows us to write mass formulas for all hydrogen nuclides considered above

$$M(^5H) = 5m_L + 14m_e + 36E_{LL} + 23E_{ee} + 35E_{Le}. \quad (9)$$

$$M(^6H) = 6m_L + 17m_e + 44E_{LL} + 25E_{ee} + 42E_{Le}. \quad (10)$$

$$M(^7H) = 7m_L + 20m_e + 52E_{LL} + 26E_{ee} + 48E_{Le}. \quad (11)$$

Table 2 shows the obtained parameters of the listed hydrogen nuclides.

Table 2

Composition of hydrogen nuclides

| Nuclide | Experiment | | Decay mode | Daughter nuclide | *LL* | *ee* | *e* | *Le* | Calculation | |
|---|---|---|---|---|---|---|---|---|---|---|
| | Mass, $m_{exp}$ (meV) | Binding energy, $E_{exp}$ (meV) | | | | | | | Binding energy, $E_{calc}$ (meV) | $\lvert E_{calc} - E_{exp} \rvert$ |
| **$^1$H** | 938.272 | 0 | Stable | | 8 | 1 | 2 | 6 | 0 | 0 |
| **$^2$H** | 1877.838 | 2.225 | n | p | 15 | 7 | 5 | 12 | 2.181 | 0.044 |
| $^3$H | 2817.403 | 8.482 | n | $^2$H | 20 | 20 | 8 | 20 | 8.466 | 0.016 |
| $^4$H | 3756.968 | 6.880 | n | $^3$H | 28 | 21 | 11 | 29 | 6.905 | 0.025 |
| $^5$H | 4696.534 | 6.680 | 2n | $^3$H | 36 | 23 | 14 | 35 | 6.731 | 0.051 |
| $^6$H | 5636.099 | 5.760 | 3n | $^3$H | 44 | 25 | 17 | 42 | 5.775 | 0.015 |
| $^7$H | 6575.665 | 5.580 | 4n | $^3$H | 52 | 26 | 20 | 48 | 6.558 | 0.022 |

**Note:** Stable nuclides are shown in bold. Source of data on masses and binding energies [38]

### *2.2 HELIUM NUCLIDES*

**Helium-3 ($^3$He).** The helium nucleus **$^3$He** (helion) arises from the $\beta$-decay of the heavy hydrogen nuclide, triton. In this case, one of the neutron electrons is emitted. This process leads to a change only in the number of electrons, leaving the number of bonds unchanged, due to the transition of one *Le*-bond to a second neutron electron. Helion, unlike triton, is stable and consists of two paired protons and one neutron (Fig. 4).

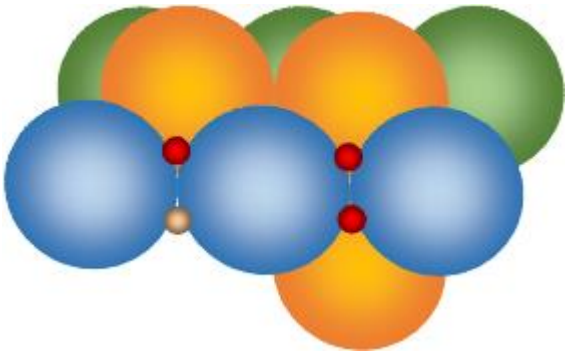

Fig. 4 – Scheme of the structure of the helion

If we assume that one of *ee*-bonds of a neutron electron are also converted into a *Le*-bond, then their number is equal to: $N_{Le}$ = 20. Accordingly, the mass formula practically coincides with the formula for triton, with the exception of the number of electrons in the nucleus

$$M(^3He) = 3m_L + 7m_e + 20E_{LL} + 20E_{ee} + 20E_{Le}. \quad (12)$$

**Helium-4 ($^4$He).** The $^4$He structure ($\alpha$-particle) is formed on the basis of the $^3$He nuclide by adding another neutron to it (Fig. 5). When performing this operation, a number of structural changes occur. Firstly, the added neutron enters into the composition of $^3$He without bound

lovetons, including only a free loveton and an electron-positron pair, which leads to an increase in the number of *LL*-bonds to the value: $N_{LL}$ = 23. In addition, we take into account the presence of pairing of protons and neutrons between themselves. This gives us 2 additional *LL*-bonds. Therefore, the total number of *LL*-bonds will be: $N_{LL}$ = 25.

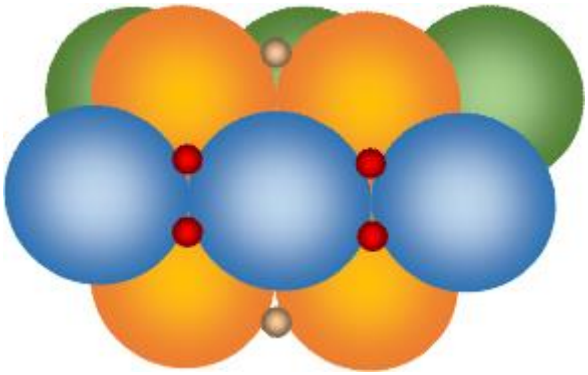

Fig. 5 – Scheme of the structure of $^4$He ($\alpha$-particle)

Secondly, the first neutron electron is displaced by the electron-positron pair of the added neutron, which contacts only one of the helium-3 electron-positron pairs, adding only three *ee*-bonds to the total number of combinations for electrons, resulting in the value: $N_{ee}$ = 18. The total number of *Le*-bonds is determined by the number of 24 given bonds between all electron-positron pairs and free lovetons, as well as bonds of neutron electrons with free lovetons, the number of which can be estimated equal to four *Le*-bonds. In this case, the total number of *Le*-bonds is: $N_{Le}$ = 28. Based on the above, we can obtain a diagram of the $^4$He nucleus, described by the mass formula

$$M(^4He) = 4m_L + 10m_e + 25E_{LL} + 18E_{ee} + 28E_{Le}. \quad (13)$$

Thus, the increased stability of an even-even system, such as α particle, can be explained both by the presence of double pairing of nucleons and by the loss of two bound lovetons.

**Helium-5 ($^5$He).** The $^5$He nuclide can be obtained by adding an additional neutron to the $^4$He nucleus. $^5$He, being an unstable nucleus by its nature, has an additive number of *LL*-bonds equal to: $N_{LL}$ =33. The number of *ee*-bonds is obtained by summing the existing bonds in $^4$He with one bond of the neutron itself and two bonds that arise during the interaction of a neutron electron with one of the electron-positron pairs of the $^4$He nuclide: $N_{ee}$ =21. The number of *Le*-bonds can also be obtained by summing up the bond data between the $^5$He nuclide and the neutron: $N_{Le}$=34.

**Helium-6 ($^6$He).** In the case of the unstable nuclide $^6$He, α particle combines with two neutrons. In this case, the core can be considered as a combined core with the loss of two *LL* connections. Summing up the number of *LL*-bonds of $\alpha$-particle and neutrons, excluding two bonds, and adding one bond that arises during neutron pairing, we finally obtain: $N_{LL}$ =40. Electron-positron pairs of neutrons and neutron electrons receive three *ee*-bonds, in the presence of the already existing 18 bonds of the $\alpha$-particle, which gives us the value: $N_{ee}$ =27. The number of *Le*-bonds is determined by summing the bonds of the $\alpha$-particle and neutrons: $N_{Le}$=40.

**Helium-8 ($^8$He).** The $^8$He nuclide is also an unstable nuclide, as is the case with $^6$He, due to its participation in $\beta$-decay processes. At the same time, this nuclide is stable with respect to *LL* bonds, which indicates its association with added neutrons. By combining $^6$He with two neutrons we also lose two *LL* bonds, but with the addition of one *LL*-bond due to neutron pairing. The calculation of the number of *ee*- and *Le*-bonds is carried out similarly to what we performed for the $^6$He nuclide.

**Helium-7,9,10 ($^{7,9,10}$He).** All helium nuclides presented here can be subject to neutron decay and, therefore, instead of combining, neutrons are added under the influence of nuclear forces. This fact allows, as in previous cases for hydrogen nuclides, to calculate the masses of nuclei by simply summing the binding energies of lovetons, electron-positron pairs, and neutron

electrons. The results of all calculations performed for helium nuclides are summarized in Table 3. For all helium nuclides with a mass number of more than four, the recording of mass formulas is carried out similarly to those performed earlier. In this work, we will not present mass formulas for unstable atomic nuclei separately due to their similarity.

Table 3

Composition of helium nuclides

| Nuclide | Experiment | | Decay mode | Daughter nuclide | *LL* | *ee* | *e* | *Le* | Calculation | |
|---|---|---|---|---|---|---|---|---|---|---|
| | Mass, $m_{exp}$ (*meV*) | Binding energy, $E_{exp}$ (*meV*) | | | | | | | Binding energy, $E_{calc}$ (*meV*) | $\lvert E_{calc} - E_{exp} \rvert$ |
| **$^{3}$He** | 2816.110 | 7.718 | $\beta^-$ | $^{3}$H | 20 | 20 | 7 | 20 | 7.684 | 0.034 |
| **$^{4}$He** | 3755.675 | 28.296 | n | $^{3}$He | 25 | 18 | 10 | 28 | 28.316 | 0.020 |
| $^{5}$He | 4695.240 | 27.560 | n | $^{4}$He | 33 | 19 | 13 | 36 | 27.536 | 0.024 |
| $^{6}$He | 5634.806 | 29.271 | $\beta^-$ | $^{6}$Li | 40 | 27 | 16 | 40 | 29.366 | 0.095 |
| $^{7}$He | 6574.371 | 28.862 | n | $^{6}$He | 48 | 31 | 19 | 44 | 28.842 | 0.020 |
| $^{8}$He | 7513.937 | 31.396 | $\beta^-$ | $^{8}$Li | 55 | 35 | 22 | 52 | 31.373 | 0.023 |
| $^{9}$He | 8453.502 | 30.141 | n | $^{8}$He | 63 | 39 | 25 | 57 | 30.243 | 0.073 |
| $^{10}$He | 9393.068 | 29.950 | 2n | $^{8}$He | 71 | 41 | 28 | 63 | 29.894 | 0.056 |

**Note:** Stable nuclides are shown in bold. Source of data on masses and binding energies [38].

### *2.3 LITHIUM NUCLIDES*

**Lithium-4 ($^{4}$Li).** The nucleus of the $^{4}$Li nuclide is formed by the addition of a proton to the helion. In this case, both data nuclides remain practically independent. The total number of *LL* links is simply summed up to give the value: $N_{LL}$ =28. Accordingly, the number of *ee*-bonds also increases by one. However, here the number of *Le*-bonds changes structurally. Six bonds from the proton structure are added to the existing 20 *Le*-bonds of the helion, and additional three *ee*-bonds of the electron-positron pair of the proton with one of the electron-positron pairs of the helion appear. A neutron electron included in the composition of a helion can also receive *Le*-bond with the proton loveton. In this case, the total number of *Le*-bonds will be: $N_{Le}$ = 30.

**Lithium-5 ($^{5}$Li).** The next nuclide $^{5}$Li additionally includes a second neutron. This makes it possible to form inside the nucleus, as one of the elements, α-particle with a proton attached to it by nuclear forces. Being, like $^{4}$Li, an unstable nucleus, this nuclide has an additive number of *LL*-bonds equal to: $N_{LL}$ =33. In the same way as in $^{4}$Li, let's sum up the number of their constituent *ee*-bonds. To the 19 existing *ee*-bonds, 2 more bonds of the electron-positron pair of the proton with a similar pair from the $^{4}$He composition will be added, which will change their number to the value: $N_{ee}$ = 21. The number of *Le*-bonds can also be obtained by summing up the data of the $^{4}$He and proton bond: $N_{Le}$=34.

**Lithium-6 ($^{6}$Li).** In the case of a stable nuclide $^{6}$Li, a deuteron is added to α particle (Fig. 6). In this case, the core can be considered as a combined core with the loss of one *LL* connection, which gives us: $N_{LL}$ =39. The number of *ee*-bonds of $^{6}$Li is determined by the number of added combinations with electron-positron pairs of the α-particle on the deuteron side, which gives 5 additional *ee*-bonds. In addition, the neutron electron retains one more bond with the electron-positron pair of the neutron, which in total leads to the value: $N_{ee}$ = 29. The number of *Le*-bonds is determined by the sum of such bonds of all elements included in the $^{6}$Li composition, with an additional bond of the neutron electron with one of lovetons. Consequently, the number of possible *Le*-bonds will be: $N_{Le}$=41.

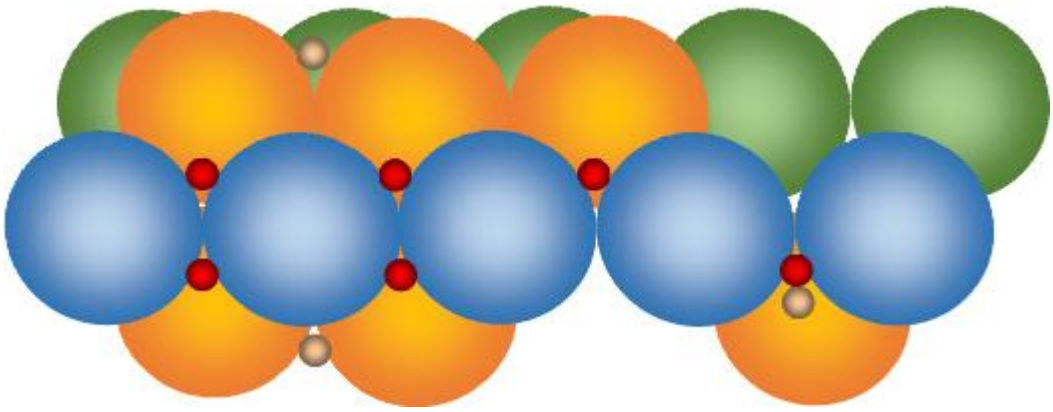

Fig. 6 – Scheme of the structure of $^{6}$Li nuclide

To calculate the mass of a stable nuclide $^{6}$Li based on the proposed structure diagram, the following mass formula can be represented

$$M(^{6}Li) = 6m_L + 15m_e + 39E_{LL} + 29E_{ee} + 41E_{Le}. \quad (14)$$

**Lithium-7 ($^{7}$Li).** The addition of the seventh nucleon in the $^{7}$Li nuclide does not change the stability of the nucleus, but at the same time leads to some change in its composition. The $^{7}$Li nuclide is α-particle combined with both a deuteron and a separate neutron (Fig. 7). In total, the number of *LL*-bonds for the $^{7}$Li nuclide increases by seven bonds and amounts to: $N_{LL}$ = 46. The number of *ee*-bonds remains the same, since taking into account the bond in the electron-positron pair is compensated by the transition of the neutron electron to bonding with the loveton. Accordingly, we get: $N_{ee}$ = 29; The number of *Le*-bonds is determined by the sum of such bonds of all nuclear elements, calculated similarly to the calculation for the previous nuclide: $N_{Le}$ = 48.

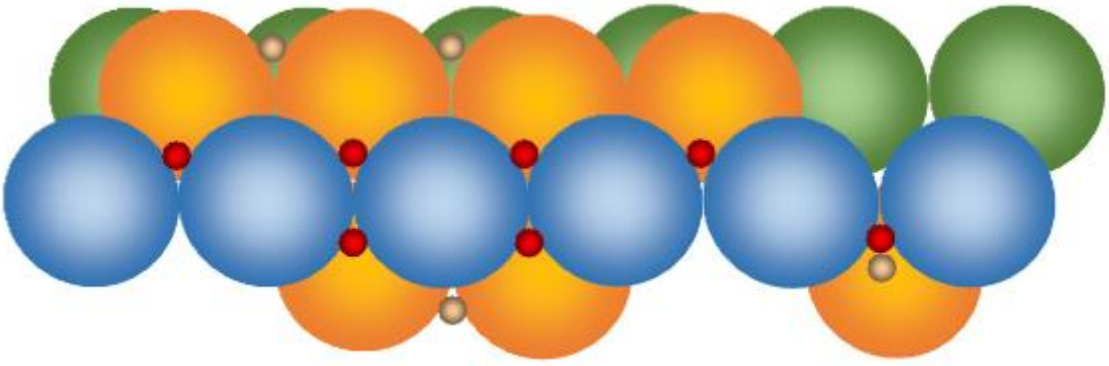

Fig. 7 – Scheme of the structure of $^{7}$Li nuclide

Here, to calculate the mass of a stable nuclide$^{7}$Li, we can write the following mass formula

$$M(^{7}Li) = 7m_L + 18m_e + 46E_{LL} + 29E_{ee} + 48E_{Le}. \quad (15)$$

**Lithium-8,9,11 ($^{8,9,11}$Li).** Nuclides $^{8,9,11}$Li are considered to be unstable due to their participation in $\beta$-decay processes. At the same time, these nuclides are stable with respect to *LL*-bonds, which indicate their association with added neutrons. Carrying out a similar examination of the structure of these nuclei makes it possible to determine the quantitative composition of these nuclides with a sufficient degree of accuracy.

**Lithium-10,12,13 ($^{10,12,13}$Li).** Regarding the nuclides $^{10,12,13}$Li, it can be argued that instead

of combining, neutrons are added under the influence of nuclear forces, which allows, as in previous cases for hydrogen and helium nuclides, to calculate the masses of nuclei by simply summing the binding energies of lovetons and electron-positron pairs , as well as neutron electrons. The results of all calculations performed are summarized in Table 4.

Table 4

Composition of lithium nuclides

| Nuclide | Experiment | | Decay mode | Daughter nuclide | *LL* | *ee* | *e* | *Le* | Calculation | |
|---|---|---|---|---|---|---|---|---|---|---|
| | Mass, $m_{exp}$ (*meV*) | Binding energy, $E_{exp}$ (*meV*) | | | | | | | Binding energy, $E_{calc}$ (*meV*) | $\lvert E_{calc} - E_{exp} \rvert$ |
| $^{4}$Li | 2816.110 | 4.600 | p | $^{3}$He | 28 | 21 | 9 | 30 | 4.559 | 0.041 |
| $^{5}$Li | 3755.675 | 26.330 | p | $^{4}$He | 33 | 21 | 12 | 34 | 26.403 | 0.073 |
| **$^{6}$Li** | 4695.240 | 31.994 | d | $^{4}$He | 39 | 29 | 15 | 41 | 32.071 | 0.077 |
| **$^{7}$Li** | 5634.806 | 39.245 | n | $^{6}$Li | 46 | 29 | 18 | 48 | 39.209 | 0.036 |
| ***$^{8}$Li*** | 6574.371 | 41.278 | $\beta^-$ | $^{8}$Be | 53 | 36 | 21 | 53 | 41.215 | 0.062 |
| ***$^{9}$Li*** | 7513.937 | 45.340 | $\beta^-$ | $^{9}$Be | 60 | 40 | 24 | 59 | 45.309 | 0.031 |
| $^{10}$Li | 9391.774 | 45.314 | n | $^{9}$Li | 68 | 41 | 27 | 66 | 45.310 | 0.004 |
| ***$^{11}$Li*** | 8453.502 | 45.709 | $\beta^-$. n | $^{10}$Be | 75 | 48 | 30 | 73 | 45.754 | 0.044 |
| $^{12}$Li | 9393.068 | 45.499 | n | $^{11}$Li | 83 | 50 | 33 | 79 | 45.579 | 0.080 |
| $^{13}$Li | 9393.068 | 45.604 | 2n | $^{11}$Li | 91 | 51 | 36 | 86 | 45.580 | 0.017 |

**Note:** Stable nuclides are shown in bold. Bold italic denotes $\beta$-decay nuclides. Source of data on masses and binding energies [38].

### *2.4 CLUSTER FORMATION OF α-PARTICLES*

The study of the static properties of compound atomic nuclei allows us to study the structural features of nuclei and the processes of their formation [39]. In carrying out this study, we will consider the problem of the formation of shells in an atomic nucleus using the example of even-even atomic nuclei. Let's take as basis even-even nuclei with the same number of protons and neutrons in the nuclei. Let us assume that collections of helium nuclei will be considered as such composite nuclei.

Before moving on to a detailed consideration of the shell model of even-even atomic nuclei, we will try to obtain quantitative estimates of the elements that make up the atomic nucleus. We will determine the number of bonds between lovetons, electron-positron pairs, as well as between electrons and lovetons by sequentially increasing them by values known for the α-particle: $N_{LL}$ = 25, $N_{ee}$ = 18, $N_{Le}$ = 28. Comparison of the obtained calculated values with known energy values connections, in order to estimate the real number of these connections, we will carry out by varying the number of connections between the individual elements that make up the core. Since the binding energy of the compound nucleus is known, changes in the composition of added $\alpha$ particle can be found by the number of *LL*-bonds of $\alpha$ particle, as well as *ee*-and *Le*-bonds. Consistent execution of this procedure, with the addition of new α-particles, allows one to perform calculations to determine the compositions of even-even nuclei from $^{4}$He to $^{100}$Sn. The results of calculations of the binding energies of such atomic nuclei are presented in Table 5.

Table 5

Cluster formation of α-particles

| Index | Nuclide | Experiment | | *LL* | $\Delta_{LL}$ | *ee* | $\Delta_{ee}$ | *Le* | $\Delta_{Le}$ | Calculation | |
|---|---|---|---|---|---|---|---|---|---|---|---|
| | | Mass, $m_{exp}$ (*meV*) | Binding energy, $E_{exp}$ (*meV*) | | | | | | | Binding energy, $E_{calc}$ (*meV*) | $\lvert E_{calc} - E_{exp} \rvert$ |
| $1s^2$ | **$^{4}$He** | 3755.675 | 28.296 | 25 | – | 18 | – | 28 | – | 28.316 | 0.020 |

| | | | | | | | | | | | |
|---|---|---|---|---|---|---|---|---|---|---|---|
| $1p^2$ | $^{8}$Be | 7511.350 | 56.499 | 50 | 0 | 37 | 1 | 55 | -1 | 56.457 | 0.043 |
| $1p^4$ | **$^{12}$C** | 11267.025 | 92.163 | 74 | -1 | 53 | -2 | 84 | 1 | 92.085 | 0.078 |
| $1p^6$ | **$^{16}$O** | 15022.700 | 127.621 | 98 | -1 | 70 | -1 | 112 | 0 | 127.539 | 0.082 |
| $1d^2$ | **$^{20}$Ne** | 18778.375 | 160.647 | 122 | -1 | 87 | -1 | 143 | 3 | 160.648 | 0.001 |
| $1d^4$ | **$^{24}$Mg** | 22534.050 | 198.257 | 146 | -1 | 105 | 0 | 167 | -4 | 198.270 | 0.013 |
| $1d^6$ | **$^{28}$Si** | 26289.725 | 236.541 | 170 | -1 | 119 | -4 | 195 | 0 | 236.593 | 0.052 |
| $2s^2$ | **$^{32}$S** | 30045.400 | 271.784 | 194 | -1 | 137 | 0 | 222 | -1 | 271.871 | 0.087 |
| $1d^8$ | **$^{36}$Ar** | 33801.075 | 306.717 | 218 | -1 | 158 | 3 | 246 | -4 | 306.623 | 0.093 |
| $1d^{10}$ | **$^{40}$Ca** | 37556.750 | 342.052 | 242 | -1 | 175 | -1 | 274 | 0 | 342.077 | 0.025 |
| $1f^2$ | ***$^{44}$Ti*** | 41312.425 | 375.475 | 266 | -1 | 195 | 2 | 301 | -1 | 375.442 | 0.033 |
| $1f^4$ | ***$^{48}$Cr*** | 45068.100 | 411.472 | 290 | -1 | 213 | 0 | 327 | -2 | 411.501 | 0.029 |
| $1f^6$ | ***$^{52}$Fe*** | 48823.775 | 447.700 | 314 | -1 | 230 | -1 | 354 | -1 | 447.736 | 0.036 |
| $1f^8$ | ***$^{56}$Ni*** | 52579.450 | 483.998 | 338 | -1 | 247 | -1 | 381 | -1 | 483.971 | 0.027 |
| $2p^2$ | ***$^{60}$Zn*** | 56335.125 | 515.004 | 362 | -1 | 267 | 2 | 411 | 2 | 514.992 | 0.012 |
| $2p^4$ | ***$^{64}$Ge*** | 60090.800 | 545.887 | 386 | -1 | 288 | 3 | 440 | 1 | 545.838 | 0.049 |
| $1f^{10}$ | $^{68}$Se | 63846.475 | 576.468 | 411 | 0 | 306 | 0 | 465 | -3 | 576.498 | 0.030 |
| $1f^{12}$ | $^{72}$Kr | 67602.150 | 606.921 | 436 | 0 | 321 | -3 | 494 | 1 | 606.902 | 0.019 |
| $1f^{14}$ | $^{76}$Sr | 71357.825 | 637.941 | 461 | 0 | 337 | -2 | 521 | -1 | 637.912 | 0.029 |
| $2p^6$ | $^{80}$Zr | 75113.500 | 669.922 | 486 | 0 | 352 | -3 | 548 | -1 | 669.879 | 0.043 |
| $1g^2$ | $^{84}$Mo | 78869.175 | 700.943 | 511 | 0 | 368 | -2 | 575 | -1 | 700.889 | 0.054 |
| $1g^4$ | $^{88}$Ru | 82624.850 | 731.464 | 536 | 0 | 386 | 0 | 600 | -3 | 731.549 | 0.085 |
| $1g^6$ | $^{92}$Pd | 86380.525 | 762.085 | 561 | 0 | 405 | 1 | 624 | -4 | 762.033 | 0.052 |
| $1g^8$ | $^{96}$Cd | 90136.200 | 793.406 | 586 | 0 | 423 | 0 | 648 | -4 | 793.474 | 0.068 |
| $1g^{10}$ | $^{100}$Sn | 93891.875 | 825.160 | 611 | 0 | 440 | -1 | 673 | -3 | 825.090 | 0.070 |

**Note:** Stable nuclides are shown in bold. Bold italic denotes not subject to nucleon decay nuclides. Changes in the number of bonds relative to the addition of an α-particle are reflected in the graphs $\Delta_{LL}$, $\Delta_{ee}$ и $\Delta_{Le}$. Source of data on masses and binding energies [38].

## *3. RESULTS AND DISCUSSION*

### *3.1 HYDROGEN NUCLIDES $^{8,9}$H*

In a previously presented article [29], it was suggested that there is a probability of population of the last two cells belonging to the *1p* subshell. In this case, it is theoretically possible to indicate the presence of hydrogen nuclides with mass numbers *A* equal to 8 and 9. When considering such hypothetical nuclides as $^{8}$H and $^{9}$H, drawing analogies with the previously considered hydrogen nuclides, it is possible to estimate not only the number of bonds formed, but also determine values of their binding energies. Here we apply two approaches simultaneously. First, let's compare the composition of the odd-even nuclides $^{4}$H and $^{6}$H with the possible hydrogen nuclide $^{8}$H, as well as the odd-even nuclides $^{5}$H and $^{7}$H with $^{9}$H. Also, to control the correctness of the assessment of data on the composition of the corresponding hypothetical nuclides, you can use linear regression equations between the quantities of *LL*-, *ee*- and *Le*-bonds and the mass number *A* of the hydrogen nuclides being determined.

***LL-bond***. When going from nuclide $^{4}$H to $^{6}$H, which have numbers of *LL*-bonds with values equal to 28 and 44, it is possible to estimate the range of data difference for the transition from nuclide $^{6}$H to $^{8}$H, which will be equal to: $\Delta N_{LL}$ = 16. In this case, the number of *LL* bonds for nuclide $^{8}$H will take the value equal to: $N_{LL}$ ($^{8}$H) = 60. In the same way, we determine the number

of *LL*-bonds during the transition from nuclide $^{7}$H to $^{9}$H: $N_{LL}$ ($^{9}$H) = 68.

To check the correctness of the above estimates, we will construct a regression equation for the dependence of the number of *LL* bonds on the mass number *A*, which can vary in the range from 4 to 7. This equation will have the form: $N_{LL} = 8A - 4$. Based on this equation, we can obtain integer values of the number *LL* -bonds are equal: $N_{LL}$ ($^{8}$H) = 60 and $N_{LL}$ ($^{9}$H) = 68, which completely coincides with the previous calculation of the considered parameters. In this case, both proposed methods are adequate, which is confirmed by the results obtained.

***ee-bond.*** We will carry out calculations to calculate the number of *ee*-connections using the same algorithm as for *LL*-bonds. First, having estimated the data difference ranges for transitions between $^{6}$H and $^{8}$H, as well as between $^{7}$H and $^{9}$H nuclides, we calculate the numbers of *ee*-bonds for selected hypothetical nuclides: $N_{ee}$ ($^{8}$H) = 28; $N_{ee}$ ($^{9}$H) = 29. Using the linear regression equation for the dependence of the number of *ee*-bonds on the mass number, which has the form: $N_{ee} = 1.6A + 15$, we obtain the values of the number of *ee*-bonds: $N_{ee}$ ($^{8}$H) = 27.8; $N_{ee}$ ($^{9}$H) = 29.4. Rounding these values to whole numbers allows you to confirm earlier calculations.

***Le-bond.*** Repeating the previous arguments for *Le*-bonds, we obtain the following values: $N_{Le}$ ($^{8}$H) = 56; $N_{Le}$ ($^{9}$H) = 62. When checking, taking into account the linear regression equation: $N_{Le} = 6.9A + 0.3$, we obtain the values of the number of *Le*-bonds: $N_{Le}$ ($^{8}$H) = 55.5; $N_{Le}$ ($^{9}$H) = 62.4. Rounding these values to integer values confirms the correctness of the calculations.

Knowing all the numerical values of the quantity *LL*-, *ee*- and *Le*-bonds, we can write mass formulas for the nuclides we considered

$$M(^{8}H) = 8m_L + 23m_e + 60E_{LL} + 28E_{ee} + 56E_{Le}. \quad (16)$$

$$M(^{9}H) = 9m_L + 26m_e + 68E_{LL} + 29E_{ee} + 62E_{Le}. \quad (17)$$

At the end of our consideration of the parameters of hypothetical hydrogen nuclides, we will evaluate their binding energies. To do this, taking the error in calculating these binding energies close to zero, for the nuclides under consideration we obtain the following values: $E_b$($^{8}$H) = 4.82 Mev; $E_b$($^{9}$H) = 5.60 Mev.

### *3.2 CHARGE RADIUS OF LIGHT NUCLIDES*

The charge radius of an atomic nucleus is one of the main parameters that determine its size and provide information about its internal structure. Let us estimate the charge radii for light nuclei of hydrogen, helium and lithium.

**Proton.** The numerical value of the proton charge radius is: $r_p$ = 0.8414 *fm* [40]. However, with previously used standard measurement methods, this indicator had a slightly different value, equal to 0.8783 *fm* [41]. Currently, it is customary to consider both of these values as acceptable when conducting research. Here, we will assume that the loveton included in the proton, in a free state or close to it, has a larger charge radius. In a state of strong connection with other nucleons, a slight decrease in the charge radius occurs. For this reason, in a number of calculations of nuclide radii, an increased value of the proton charge radius (deuteron, triton and helion) will be used; in other cases, a refined value of this parameter will be used.

**Deuteron.** The known value of the deuteron charge radius is equal to 2.1424 *fm* [42]. The charge radius of the deuteron can be calculated using a scheme with diagonal placement of lovetons (Fig. 2b). In this case, we will assume that the axis of charge symmetry *OO′* is located strictly between these particles, perpendicular to the line connecting the centers of free lovetons (Fig. 8).

In this case, the charge radius of the deuteron can be calculated using the formula: $r_d = r_p(\sqrt{2} + 1)$. Calculation using this formula gives the deuteron radius a value of 2.1185 *fm*.

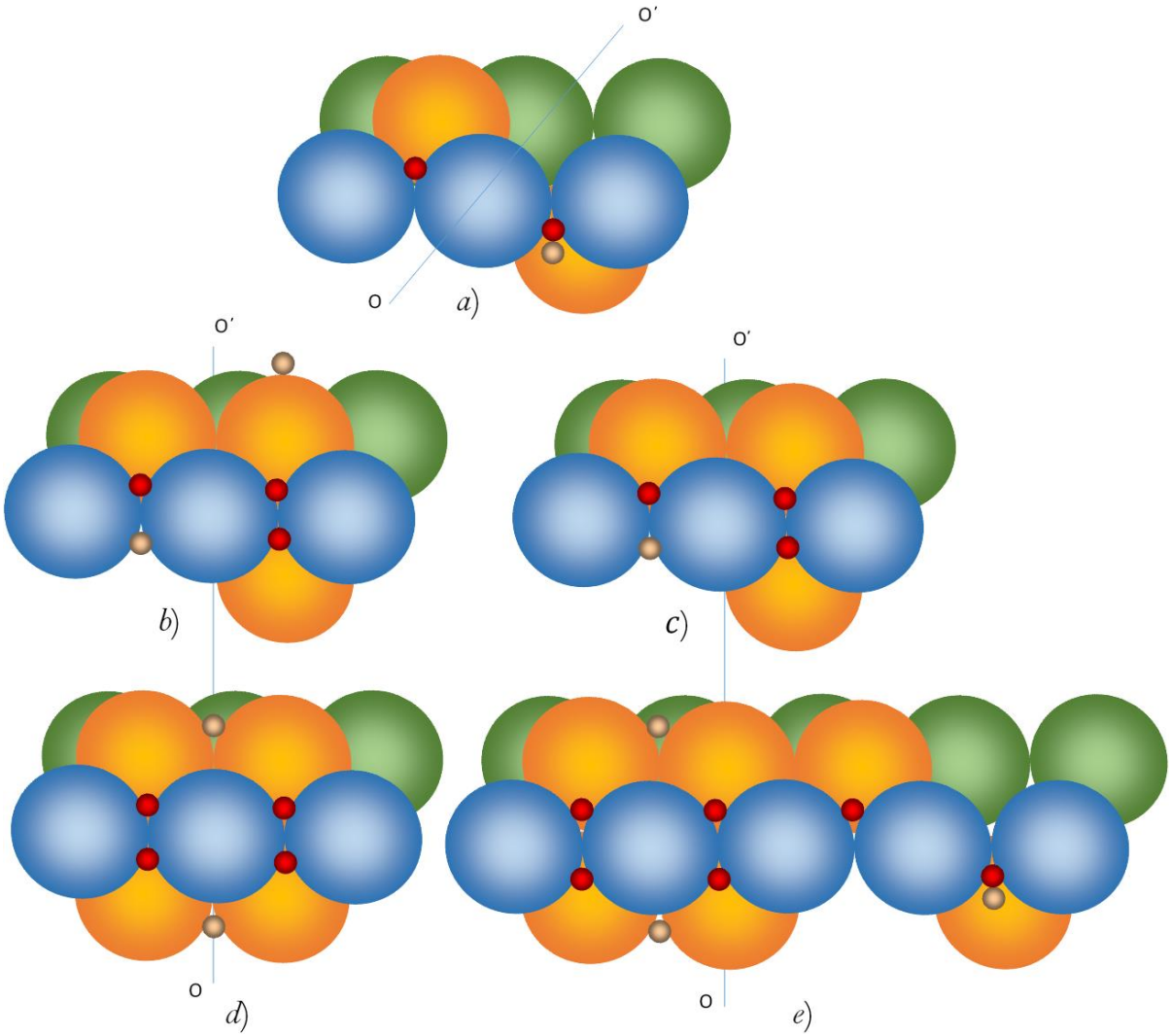


Fig. 8 – Charge radii of light nuclides:
*a*) deuteron; b) triton; c) helion; d) helium-4; *e*) lithium-6. *OO′* – axis of charge symmetry

**Triton.** Now let's move on to the triton. Here we will place the axis of charge symmetry in the vertical direction (Fig. 8). The experimental value of the triton radius is: $r_t$ = 1.7591 *fm* [42]. The absence of electrostatic interaction allows, as in the case of the deuteron, to calculate the charge radius of the triton, taking into account the occurrence of nuclear rotation along the axis of charge symmetry passing along the OO′ line. In this case, the triton radius can be taken equal to double the proton radius: $r_t = 2r_p$ = 1.7550 *fm*, which practically coincides with the value obtained experimentally.

**Helion.** Let us determine the charge radius of the helion (Fig. 8). To determine the charge radius, we first estimate the distance between the proton centers. Considering that the equality of nuclear and Coulomb forces will occur at $\Delta r = l\sqrt{6}$ ($\Delta r$ – is the distance between the centers of protons; l is the arm of the dipole represented by the electron-positron pair) [37]. If we consider the dipole arm to be numerically equal to the proton radius: $l = r_p$, then the value of $\Delta r$ will be a distance of the order of 2.1494 *fm*. In this case, the helion's charge radius will take a value equal to 1.9522 *fm*, which is quite close to the experimental value of 1.9661 *fm* [42].

**Helium-4.** During the transition from helion to helium-4, the charge symmetry axis retains its position (Fig. 8). Here it should be assumed that the charge radius of this nucleus should be equal to twice the radius of the proton. At the same time, the protons themselves included in the nucleus must be considered significantly more strongly bound, which leads to the absence of changes in their positions and the need to take into account the current value of their charge radius, equal to 0.84184 *fm*. In this case, the charge radius of helium-4 has a value of 1.67824 *fm*. This

value practically coincides with the double charge radius of the proton.

**Lithium-6.** The root mean square charge radius of $^{6}$Li is usually estimated as follows: $r_{Li}$ = 2.589 *fm* [33]. Just as for helium-4, we take the charge radius of the proton to be equal to: $r_p$ = 0.84184 *fm* [32].

We will calculate the charge radius of lithium-6 taking into account the displacement of the charge symmetry axis by the value of the proton radius (Fig. 8). In Figure 8 the axis of charge symmetry already passes through the lovetons centers. The right-handed loveton included in the neutron does not affect the value of the charge radius. In this case, the charge radius of this nucleus must be equal to triple the radius of the proton. Calculation of the charge radius of lithium-6 shows a value equal to: $r(^{6}\text{Li})$ = 2.5525 *fm*. The absolute error, when comparing the calculated value of the charge radius with the experimental one, does not exceed a value equal to 0.07 *fm*.

The charge radius of lithium-7 can be estimated similarly. However, due to the influence of strong interaction, the radius may have a slightly smaller value. At this stage of the study, this calculation was not carried out. All data on the charge radii of light nuclides are presented in Table 6.

Table 6

Charge radii of light nuclides

| Nuclide | Experimental value, $r_{exp}$ | Calculated value, $r_{calc}$ | $\lvert r_{exp} - r_{calc} \rvert$ |
|---|---|---|---|
| Deuteron, $^{2}$H | 2.1280 | 2.1185 | 0.0095 |
| Triton, $^{3}$H | 1.7591 | 1.7550 | 0.0041 |
| Helion, $^{3}$He | 1.9661 | 1.9522 | 0.0139 |
| Helium-4, $^{4}$He | 1.6755 | 1.6837 | 0.0082 |
| Lithium-6, $^{6}$Li | 2.5890 | 2.5255 | 0.0635 |

As can be seen from Table 6, the calculated values the charge radii of the nuclides practically coincide with the experimental values of the considered light nuclei, which indicate the validity of the proposed visual model of the atomic nucleus.

### *3.3 CLUSTER AND SHELL MODELS FOR α-PARTICLES*

From the data shown in Table 5, it is clear that the $^{8}$Be nucleus, in which the forces of electrostatic interaction prevail over nuclear forces, can be stated to be independent of each other, the two alpha particles included in its composition. Here one $\alpha$ particle occupies the *1s* level, while the next one occupies the higher *1p* state. Subsequently, in accordance with the selected layers of the core shell, at each step of the proposed procedure, all nuclei from $^{12}$C to $^{64}$Ge sequentially lose one *LL* connection. It can also be noted that the spatial distributions of $\alpha$ particles in nuclei do not have an *LL* relationship between individual orbitals.


Fig. 9 – Spiral form of representation of the shell structure of the core

In this case, neighboring clusters, in the form of $\alpha$-particles, can have a number of *ee*- and *Le*-bonds with each other. This fact indicates the possibility of considering the visual arrangement of $\alpha$-particles not as a set of shells, but as a set of spirals when considering each of the orbitals of the nucleus (Fig. 9). Subsequent nuclei, starting with the $^{68}$Se nuclide, are already attached without changing the number of *LL*-bonds and, therefore, with a predominance of nuclear forces, during their formation, over the bonds between nuclear elements.

To summarize, we note that from the point of view of the proposed approach, even-even atomic nuclei can be considered as a system of helium nuclei strongly bound to each other within individual orbitals of a compound nucleus. Thus, in space, the configuration of $\alpha$-particles should not look like a set of shells, but can be considered as a group of spirals.

## *4. CONCLUSION*

In contrast to previously proposed approaches to calculating the binding energy of a nucleus, the representation of clusters in the form of a collection of light nuclei and individual nucleons made it possible to construct visual structural objects that explain not only the reason for the occurrence of binding energy, but also the patterns of hydrogen, helium and lithium nuclides. In the proposed cluster model, it is possible to well reproduce such static characteristics of nuclei as nuclear masses, their binding energies, as well as quantitative values of such quantities as the number of nuclear elements that make up the selected nuclide. Thus, we have shown that the previously expressed assumption about the existence of nuclear elements allows you to simulate the dependence of binding energy on the number of nucleons. The disadvantage of the developed model compared to the semi-empirical droplet model is that the model parameters are determined not for the entire set of nuclides at once, but for the nuclides of each element separately. The advantage here is a clearer physical meaning of the parameters included in the mass equations. The main result of this work is that a model has been obtained that describes the relative arrangement of lovetons, neutron electrons and electron-positron pairs in the nucleus. In accordance with the proposed model, the structure of atomic nuclei is mainly formed due to *LL*-bonds formed as a result of the interaction of both bound and free lovetons.

Using the presented approach, the following results were obtained:

1. All nuclei are constructed by taking into account the interaction of both free and bound lovetons, forming a quasicrystalline spatial structure.

2. The nature of the appearance of nuclear binding energy, which arises due to the breaking of some of the bonds between nuclear elements, has been revealed.

3. The reason for the change in the properties of nuclei during transitions from even to odd nuclei has been clarified.

4. The main contribution to the mass comes from the binding energy of Lovetons. An additional contribution to the mass of the nucleus is the binding energy between electron-positron pairs, neutron electrons and their interaction with lovetons.

5. Nuclear diagrams were constructed and the masses and binding energies of light nuclei were calculated.

6. The binding energies for hypothetical nuclides $^{8}$H and $^{9}$H were determined.

7. The charge radii of a number of light nuclides were calculated.

8. Clustering of nucleon systems for light and medium nuclei, represented by collections of α-particles, has been carried out. Obtained estimates of binding energies for even-even nuclides with $Z=N$ for mass numbers in the range $4 \geq A \leq 100$ using an analysis of the behavior of the relationships between the number of nuclear elements and mass numbers.

9. The possibility of a spiral form of representation of the shell structure of the nucleus is shown, i.e. in the form of a set of spirals.

The application of the proposed method for describing the masses of atomic nuclei has shown that estimates of the parameters under study obtained with its help are sufficiently accurate, and the method itself is simple both in calculations and in the clarity of the results obtained. The presented model of the atomic nucleus can also be useful in calculating the binding energies of nuclides when also considering heavy nuclei.

### *References*


1. Littlefield T. A. Atomic and nuclear physics. – New York: Springer US, 2014. – 487 p.
2. Kragh, H. Nuclear physics in the twentieth century: Historical and philosophical reflections. – Princeton: Princeton University Press, 2002. – 494 p.
3. Ishkhanov B.S., Kapitonov I.M., Yudin N.P. Particles and atomic nuclei. – M.: LKI Publishing House, 2019. – 672 p. (in Russian).
4. Neuchudin V.G., Smirnov Yu.F. Nucleon associations in light nuclei. – M.: Nauka, 1969. – 413 p. (in Russian).
5. Wildermuth K., Tang Y.C. A unified theory of the nucleus. – Vieweg. Braunschweig, 1977. – 389 p.
6. Hofstadter R., The structure of nuclei and nucleons // Science, 1962, Vol. 136. – PP. 1013-1022.
7. Goeppert-Mayer M., Jensen J.H.D. Elementary theory of nuclear shell structure. –New York: Wiley, 1955. – 296 c.
8. Goriely S., Tondeur F., Pearson J. M. A Hartree-Fock nuclear mass table // At. Data Nucl. Data Tables. – 2001. – Vol. 77, No 2. – PP. 311–381.
9. Sobiczewski A., Litvinov Yu.A., Palczewski M. Detailed illustration of accuracy of presently used nuclear-mass models // Atom. Nucl. Data Tables. 2018. V. 119. P. 1-32.
10. Lunney D., Pearson J.M., Thibault C. Recent trends in the determination of nuclear masses // Rev. Mod. Phys. 2003. V. 75. No. 3. P. 1021-1082
11. Samyn M., Goriely S., Pearson J. Further explorations of Skyrme–Hartree–Fock–Bogoliubov mass formulas // Nucl. Phys. A., 2003, Vol. 725. – PP. 69–81.
12. Goriely S., Chamel N., Pearson J.M. Further explorations of Skyrme-Hartree-Fock-Bogoliubov mass formulas // Phys. Rev. C., 2013, Vol. 88, No 2. – PP. 1–14.
13. Kurgalin S.D. Neutron clusters in nuclei / S.D.Kurgalin, Yu.M.Chuvilsky // Izv. AN. Ser. phys., 2003, Vol. 64, No. 5. – PP. 700-703 (in Russian).
14. Rodkin D.M., Chuvilsky Yu.M. Description of cluster phenomena in the spectra of light nuclei within the framework of the ab initio approach // Letters in the JETF, 2018, Vol. 108(7). – PP. 459-465 (in Russian).
15. Kadmensky S.G., Kadmensky V.G. Cluster Degrees of Freedom and Nuclear Reactions and Decays // Cluster Phenomena in Atoms and Nuclei. B. – Springer, 1992. – PP. 525-539.
16. Bettini A. Introduction to Elementary Particle Physics. – Cambridge: University Press, 2008. – 447 p.
17. Jolos, R.V. Models of atomic nuclei. – Dubna, OIYAI, 2012. – 107 p. (in Russian).
18. Ishkhanov B.S. Atomic nuclei // Physical Bulletin of the Moscow University. - 2012, Volume 67. – pp. 1-24.
19. Rowe D.J., Wood J.L. Fundamentals of nuclear models: foundational models. World Scientific, Singapore, 2010. – 676 p.
20. Kislov A.N. Atomic and nuclear physics. Yekaterinburg: Ural Publishing House. unita, 2017. – 271 p. (in Russian).
21. Nemirovskii P.E. Contemporary models of the atomic nucleus. – New York: Elsevier, 2013. – 344 p.
22. Calculator and Graph Engine for Atomic Nuclei Parameters / The Centre for Photonuclear Experiments Data of the Moscow State University. Access mode: URL: http://cdfe.sinp.msu.ru/services/calc_thr/calc_thr.html.

23. Myers W.D., Swiatecki W.J. Nuclear masses and deformations // Nucl. Phys., 1966, Vol. 81, No. 1. – PP. 1-60.
24. Wigner E. On the Consequences of the Symmetry of the Nuclear Hamiltonian on the Spectroscopy of Nuclei // Phys. Rev., 1937, Vol. 51, No. 2. – PP. 106-119.
25. Wong S.S.M. Introductory Nuclear Physics. – WILEY-VCH Verlag Gmbl I & Co. KGaA, Weinheim, 2004. – 473 p.
26. Garvey G.T., Kelson I. New nuclidic mass relationship // Phys. Rev. Lett. 1966. Vol. 16. – PP. 197-200.
27. Möller P., Nix J.R. Nuclear mass formula with a finite-range droplet model and a folded-Yukawa single-particle potential // At. Data Nucl. Data Tables, 1988, Vol. 39, No. 2. – PP. 225-233.
28. Möller P., Sierka A.J., Ichikawab T., Sagawac H. Nuclear ground-state masses and deformations: FRDM (2012) // At. Data Nucl. Data Tables, 2016, Vol. 109/110. – PP. 1-204.
29. Migal L.V., Bondarev V.G. Computer visualization of the spatial structure of the atomic nucleus // Research result. Information technologies. – T.7, №2, 2022. – PP. 3-18 (in Russian).
30. Rainwater J. Background for the spheroidal nuclear model proposal. – Nobel Lecture, Stockholm, 1975. – PP. 1-13.
31. Cook N.D. Models of the atomic nucleus: unification through a lattice of nucleons. – Springer-Verlag: Berlin, Heidelberg, 2006. – 291 p.
32. Nasser G.A. Body-centred-cubic (BCC) lattice model of nuclear structure. Access mode: URL: https://vixra.org/pdf/1312.0184v1.pdf
33. Feldman G. Why neutrons and protons are modified inside nuclei // Nature, 2019, Vol. 566, No. 7744. – P. 332-333.
34. Wildermuth K., Tang Y.C. A unified theory of the nucleus Braunschweig, 1977. – 389 p.
35. Solovyov V.G. Theory of the atomic nucleus: Nuclear models. – M.: Energoatomizdat, 1981. – 296 p. (in Russian).
36. Ishkhanov B.S., Stepanov M.E., Tretyakova T.Y. Pairing of nucleons in atomic nuclei // VMU. Series 3. Physics. Astronomy, 2014. No. 1. – pp. 3-19. (in Russian).
37. Bondarev V.G., Migal L.V. Computer modelling of material objects' structure. Part II. Elementary particles // Research result. Information technologies. – T.8, №1, 2023. – P. 3-22. (in Russian).
38. Wang M. The AME 2020 atomic mass evaluation (II). Tables, graphs and references // Chinese Phys. C, Vol. 45, No. 3, 2021. – 513 p.
39. Bohr A., Mottelson B.R. Nuclear structure. Vol. 1. Single-particle motion. – New York: W.A. Benjamin, Inc., 1969. – 471p.
40. NIST Handbook of Constants, Units of Measurement and Uncertainties. – Access mode: URL: www.nist.gov.
41. Khabarova K.Yu., Kolachevsky N.N. The charge radius of a proton // UFN, 2021, Vol. 191, No. 10. – PP.1095-1106. (in Russian).
42. Agneli I., Marinova K. P. Table of experimental nuclear ground state charge radii: An update // At. Dat. Nucl. Dat. Tab. 2013, Vol. 99, No. 1. – PP. 69-95.